**Journal of Multidisciplinary Engineering Science and Technology (JMEST)**
**ISSN: 3159-0040**
**Vol. 2 Issue 11, November - 2015**

# 2D Controlled Source Seismic Mapping Of The Low Velocity Layer In Magadi Basin, Kenya

**Mulumbu Elly B. K'orowe Maurice O. and Githiri John G.**
Department of Physics.
Jomo Kenyatta University of Agriculture and Technology,
Nairobi, Kenya.
*(ellybogi@gmail.com , modondi@yahoo.com and githiri@fsc.jkuat.ac.ke)*

***Abstract*—2D controlled source shallow seismic refraction survey was carried in Magadi basin to determine the characteristics of the low velocity zone. These characteristics involved determining the velocities and thicknesses of various layers in the low velocity layer (LVL) using the refracted arrivals. These survey involved using critically refracted arrivals assuming a flat layer model to determine the velocity and the thickness of the weathering layer at each station. The thicknesses and velocities obtained are useful in delineating the extent of the low velocity layer suitable for determining static corrections necessary in a reflection survey devoid of anomalous effects of the low velocity layer. The data was collected using 1C-24 channel geophones of 10Hz at an interval of 3 km. The length of the spread was 108m long with a sledge hammer as a source of seismic waves. Data was recorded in SEG-Y format then transcribed to 2D/3D Vista Seismic Processing software for first break picking. Picked first break time were loaded into spreadsheet where layers were picked and velocities calculated using time intercept method. A two layer model of the weathered zone was observed and 2D LVL modeled on each profile to show the trend of the weathering zone in Magadi basin**

***Keywords— Magadi Basin, seismic refraction, low velocity layer, Intercept time method***

## I. INTRODUCTION

The near surface seismic waves can provide useful information about near surface characteristics whose velocities and depths are generally unknown. However, separate refraction or uphole survey can be carried out prior to deep seismic reflection survey to understand its anomalous behavior, useful in processing deep reflection seismic data. In Magadi basin, shallow seismic refraction or uphole survey has not been done. However, large scale seismic refraction profiles were recorded across the region by the Kenya Rift International Seismic Project (KRISP) in 1987 [1] and 1990. The data provided a good picture of the overall crustal structure of the region. Mechie et al., [2] observed that the variation of the crustal structure across the rift are surprisingly large, generally correlating with the elevation of the Rift Valley floor. In the southern part, the seismic P-wave velocity information showed that the crustal boundary outside the rift occurs at 42km depth. Bonjer et al., [3], Backhouse and Long [4] discovered that low P-waves velocities (7.5-7.7km/s) have been detected below the rift, while outside the rift, P-wave velocities appear normal i.e. 8.0-81km/s. Most of the seismics survey carried out were for mapping the crustal structure and the mantle of the earth. Githiri, [5] studied the depth to basement using gravity and magnetic surveys for locating a geothermal reservoir. However, this paper is focused on studying characteristics of the weathered zone that has great impact in processing deep reflection seismic data for locating geological features necessary for hydrocarbon location.

The low velocity layer (LVL) zone has various properties. It is usually aerated, loose, unconsolidated with abnormally low velocities, variable thicknesses, densities and lithologies. It is characterized by low transmission of seismic waves and shots taken in this layer tend to be of low frequencies as the layer is capable of absorbing high frequency signals. Datuming through an incorrect weathering model can introduce false structures in the deep reflectors [6]. The number of refractors (layers) present in the weathering zone can be determined explicitly by examining the differences between first-arrival travel times on records from overlapping spreads. Rather than finding velocities and thicknesses of layers, shallow seismic refraction data is commonly used in oil and gas exploration with the aim of computing static correction for seismic reflection surveys. The static corrections obtained are used to adjust travel times passage for seismic waves through the thick, low velocity layer "weathered zone" overlying solid rock. Lawton [7] observed that absolute values of the static corrections were less than 10ms, had greater effect on reflection travel times than does the surface topography and increased in response to the increasing thickness of glacial overburden in Southern Alberta, Calgary.

In 2012, Kolawole et al., [8] analyzed downhole refraction in Niger Delta Basin and observed an irregularity caused by faulting along the true base of weathering. Saha et al., [10] investigated the velocity and depth of the weathered layer using a downhole seismic refraction technique in Assam Basin in Nigeria in 2012. Analysis of velocity-thickness map of all the layers in Assam Basin area showed significant variations in local and regional scales of LVL near Naga thrust area. In this study, use is made first breaks to determine the average velocities, thickness of the weathered zone and number of layers to the bedrock in Magadi basin. Finally, using the thicknesses obtained, a comparison of depth is made with other geophysical studies carried out in the area to determine the depth to the consolidated zone.

### A. Area of Study and Geology

Magadi basin is located in Kajiado County, approximately 100km from Nairobi in the southern part of Kenya as shown in Fig. 1. The area is bounded by latitudes $1^0$ 40'S and $2^0$ 10' S and Longitudes $36^0$ 00' E and $36^0$ 30' E. It is in the southern part of the Gregory Rift of continental type. It extends from the Magadi to Natron, a quaternary basin in the south of Baringo and Suguta grabens in the north; a complex grabens bisecting the Kenya domal uplift [5]. The lake Magadi is located in a broad flat depression with the lowest point in the Southern part of the Kenya Rift Valley.

### B. Geology of the Study Area

The Magadi basin is classified into three formations by Baker [11], [12] namely Precambrian metamorphic rocks, Plio-Pleistocene volcanics, the Holocene to recent lake and fluvial sediments. The basement rocks outcrop in the region west of the Nguruman escarpment. These rocks consist mainly of regular banded schists, gneisses and muscovite-rich quartzites (Fig. 2). Baker [11] found that the olivine basalt layers of the Kirikiti platform are interbedded with conglomerates; gravels and sands deposited between different eruption episodes. Three central volcanoes exist; olorgesailie, Oldoinyo Nyokie and Shompole as illustrated in Fig. 1. Olorgesailie is the highest. Its lava composition consists of olivine basalts, alkali trachyte and nephelinite. Further south, the Lenderut volcano dated 2.5 Ma has basalt and andesite lavas, while Shompole dated 2.0 Ma consists of carbonates and nephelinite rocks [12]. Crossley, [13] found that the most extensive volcanic activity in the area occurred between 1.4 and 0.7 Ma. During this period the Magadi Trachyte series were formed and consisted of alkali lava sheets extending many kilometers that overlie most of the volcanics in the area. Magadi trachytes were followed by development of ash and lava vents and small obsidian lava volcano Oldoinyo Nyokie marking the end of volcanism in the southern Kenya Rift.

Lacustrine and fluviatile sediments were last geological formations. Lake bed lay in the bottom of fault troughs and depressions mostly covered by alluvial silts, clays and boulder beds. These are exposed around Lake Magadi mainly in the Eastern trough of the lake. The fluviatile sediments are mainly located in the Ewaso Ngiro Basin. Other superficial deposits are the alluvium and soil filled Kordjya basin and Kora Basin [11]. The Magadi area is largely covered by quaternary sediments that overlie extensive Pleistocene lavas. The trachyte lava overlies Pliocene olivine basalts and nephelinites that rests on the archean basement. A dense network of grid faults trending in the north south have created fault scarps that has affected the area and control the occurrence of geothermal manifestations as observed by Riaroh and Okoth, [14]. Fig. 2 shows the geology of the study area.

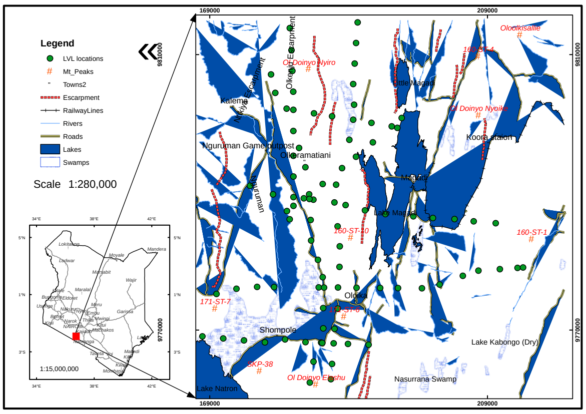


**Fig. 1**: *The study area of Magadi basin showing seismic refraction locations*

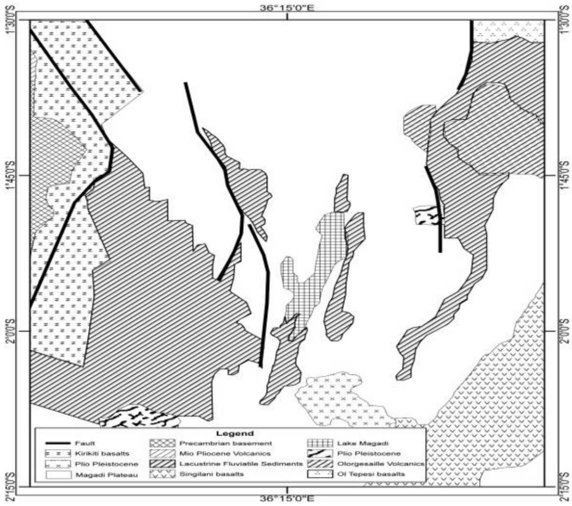


**Fig. 2:** *Geological map of Magadi area, [5]*

## II. MATERIAL AND METHODS

### Field Work and Data Acquisition

LVL refraction seismic data was acquired in 92 stations at an interval of 3km in eight transects (Fig. 3). The spread length was 108m with a minimum offset of 20cm. 24 channel receivers at each station coupled firmly in the ground were used to record the shallow seismic waves. Sledge hammer was used as a source of seismic waves. DAQLink III received analogue seismic signals, converted them to digital signal and displayed to the computer. 10-15 shots was made for forward and reverse shooting to minimize background noise effects and to also increase signal to noise ratio for clarity of first breaks. Quality control was done during recording to eliminate noise/unwanted signals to ensure the signals recorded were of good quality.

A sampling rate of 125μs and a recording length of 500ms was used. The spread configuration at each station was 1m-2m-2m-3m-3m-5m-5m-6m-6m-8m-8m-10m-8m-8m-6m-6m-5m-5m-3m-3m-2m-2m-1m. Data was recorded to Vscoope database and exported to SEG-Y file. The exported SEG-Y files were transcribed to Vista 2D/3D Software version 9.0 for processing and first break picking.

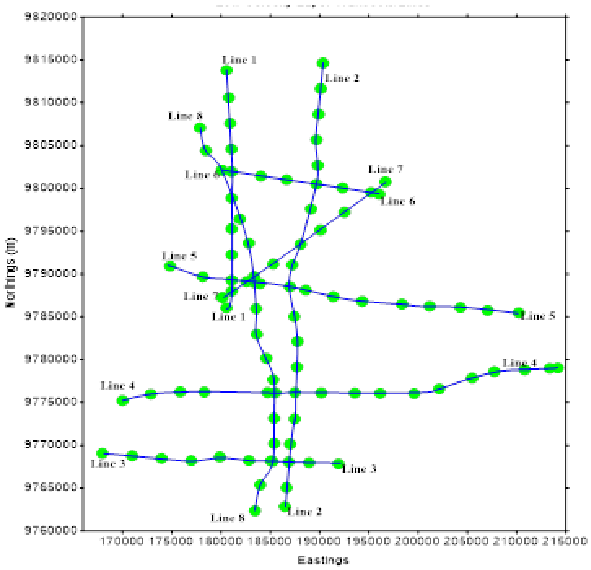


**Fig. 3**: *Location of shallow refraction seismic stations and transects/lines of data acquisition.*

The 10-15 forward shots were stacked into a single datum of 24 traces and first break time picking done. This process was then repeated for reverse shots. The first break times picked for forward and reverse shooting were loaded into spreadsheet where layers were picked and velocities calculated (Fig. 4). The picked travel times were plotted against the source-receiver distance. The slope of each of the three layers were used to determine the velocities of each layer as explained in the next section.

## III. DATA ANALYSIS

For a typical seismic source, the direct ray travels along a straight line of distance, X to the detector at velocity $V_0$. The travel time of direct ray is given by (1).

$$t_{direct} = X/V_0 \quad (1)$$

Keary et al., [15] defines (1) as a straight line slope passing through the origin of the time-distance (T-X) graph. The inverse of the slope of the T-X graph gives the velocity of the first layer. Subsequently, the inverse of the second layer and third layer are the velocities of the second and the third layer respectively. The thickness $Z_0$ and $Z_1$ are deduced from the point of intersection (inflexion point) of the two layers using (2) and (3) of time intercept method.

$$Z_0 = \frac{t_0}{2}\left(\frac{V_1 V_0}{\sqrt{V_1^2 - V_0^2}}\right) \quad (2)$$

$$Z_1 = \frac{1}{2}\left[t_1 - \frac{2Z_0\sqrt{\left(V_2^2 - V_0^2\right)}}{V_2 V_0}\right]\frac{V_2 V_1}{\sqrt{\left(V_2^2 - V_1^2\right)}} \quad (3)$$

Where: $t_0$ and $t_1$ are the intercept times on the time - distance graph. $V_0$, $V_1$ and $V_2$ are the velocity of the weathered zone, semi-weathered zone and the bedrock/consolidated zone respectively. The total thickness of the weathering zone is given by (4).

$$Z_W = Z_0 + Z_1 \text{(m)} \quad (4)$$

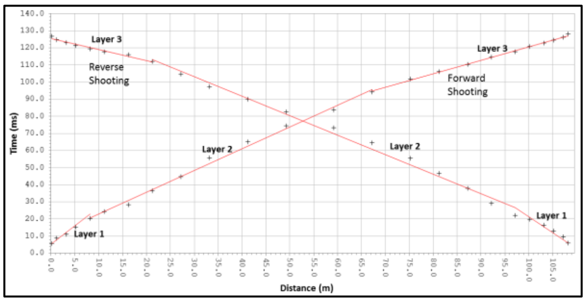


**Fig. 4:** *LVL datum for line 1 station 8 showing time-graph plot for forward and reverse shooting.*

By application of (1), the reciprocal of the slopes for each layer (Fig. 4) gives velocity of the first, the second and third layer of this station as 358.089m/s, 785.61m/s and 1265.34m/s respectively. Intercept times formula's (2) and (3) were applied to calculate the thickness of the first layer and second layer respectively. The thickness were found to be 2.1m and 20.8m respectively; giving a total depth 22.9m to the bedrock for forward shooting. A repeat was done for reverse shooting and the velocities of 422.11m/s, 879.12m/s and 1552.31m/s were obtained for first, second and third layer respectively while thicknesses of 3.4m and 29.7m were obtained for first and second layers respectively. A total thickness of 33.1m to the consolidated zone was obtained for reverse shooting. These are apparent velocities and apparent depths for each of the layers. Knodel et al., [16] suggests to determine true velocities and depths of layers, an average of the velocities and thicknesses for forward and reverse shots be done to obtain the true velocities and depths of each layer for each station. This was done for each of the stations (Fig. 3) and results summarized in Table 1. The results obtained for reverse and forward shooting, were used to create a 2D model to show the trend of different layers on each station by assuming a flat layer model, (Fig. 5).

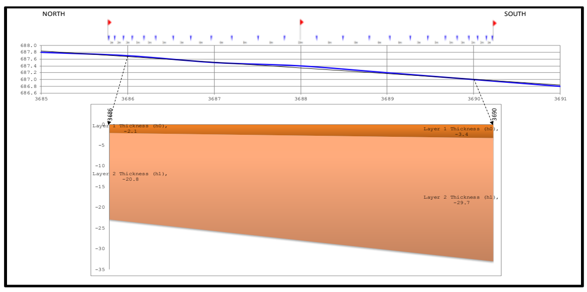


**Fig. 5**: *2D model of the refractive survey for Station 8*

Table 1: LVL interpretation for velocity and thickness for forward and reverse shooting

| | Velocity, V (m/s) | | |
|---|---|---|---|
| | $V_0$ | $V_1$ | $V_2$ |
| **Forward Shooting** | 358 | 786 | 1265 |
| **Reverse Shooting** | 422 | 879 | 1552 |
| **Average Velocity** | 447.1 | 832 | 1408.8 |
| | **Thickness, Z (m)** | | |
| **Thickness** | $Z_0$ | $Z_1$ | $Z\ (Z_1+Z_0)$ |
| **Forward shooting** | 2.1 | 20.8 | 22.9 |
| **Reverse Shooting** | 3.4 | 29.7 | 33.1 |
| **Average Thickness** | 2.7 | 25.3 | 28 |

**$V_0$**- velocity of layer 1, **$V_1$**- velocity of layer 2, **$V_2$**-velocity of layer 3. **$Z_0$**-thickness of layer 1, **$Z_1$**- thickness of layer 2, **Z**-total thickness of layer 1 and 2.

Fig. 5 shows the spread of 108m and display of geophones on this station at the top. Below it, is a graph showing the variation of topography along this station. 2D model refractive survey assuming a flat layer for this station is shown at the bottom. From Fig. 5, the elevation decreases towards the South. It's also observed that, the depth of both the first and the second layer increases towards the south. The first layer lies is observed to have an average thickness of 2.7 m. Below this layer, is a second layer of an average thickness of 25.3 m. Sum of this two thickness of the two layers gives an average thickness of the weathered zone to the bedrock as 28.0m.

## IV. RESULTS AND DISCUSSION

After analyzing the results for each station in Table 1, a 2D variation of LVL along each of the eight lines was modeled along each of the profiles (Fig. 3). Seismic refraction lines 1, 2 and 8 are oriented in N-S direction while line 7 is oriented in NE-SW direction, (Fig. 3). The elevation of these lines (Fig. 6, Fig. 7 and Fig. 8) decreases towards the south with highest elevation in the North. Line 7 (Fig. 9) has fairly constant altitude with slight increase at station 4.

The LVL of line 1 (Fig. 6) has an average velocity of 263m/s and 1068m/s with average thicknesses of 2.2m and 21.3m for layer 1 and layer 2 respectively. Layer 1 of line 1 is thick between stations 1 and 9 while thicker between stations 15 to 21. Station 9 and 13 have the minimum depths. Layer 2 is thicker than layer 1 with maximum thickness observed at station 11.

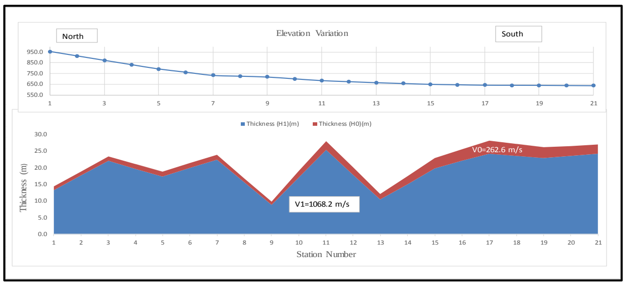


**Fig. 6**: *2D LVL variation along line one.*

The LVL of line 2 (Fig. 7) is quite intermittent. Layer's 1 and 2 have velocities of 335.7m/s and 1323.8m/s with thicknesses of 3m and 26.4m respectively. The average depth of this line is 29.4m. Maximum depths are observed from stations 8-13 with lowest depths seen at stations 8 and 15. The large thicknesses from stations 8-13 (Fig. 7) observed are within the basin where erosion of trachytes, alluvial silts by wind and water are deposited in the lowland regions resulting in increase in depth of LVL. Line 8 (Fig. 8) is the second longest line in N-S direction and has average velocities of 217.7m/s and 878m/s for layer 1 and 2 respectively. These velocities are well within a weathering zone. The average thickness of layer 1 is 2.4m and 22.1m for layer 2. Layer 1 thickness is generally constant along line 8. Maximum thickness of LVL is observed between stations 8-14 while station 5 has the lowest depth.

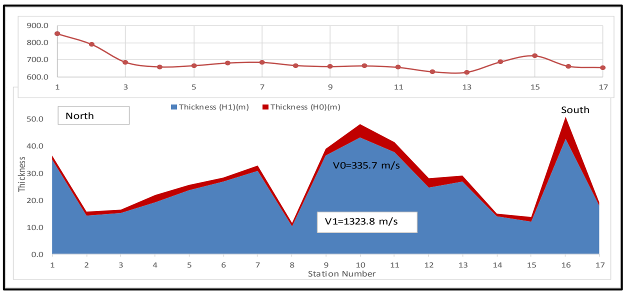


**Fig. 7**: *Variation of LVL layer and topography along line 2*

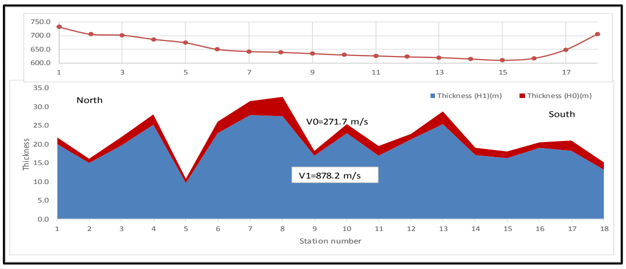


**Fig. 8**: 2D LVL Variation along line 8

Line 7 (Fig. 9) has generally constant elevation except at station 4. Similarly, the LVL layer is fairly constant except at station 4 which has the minimum thickness. The least thickness at this station could be attributed to erosion of the weathering zone due to surface run off and wind erosion towards Lake Magadi since it is highly elevated. The thickness of layer 1 increase towards SW as seen in Fig. 9. Layer's 1 and 2 are generally constant except at station 4. Layer 1 and 2 have average velocities of 274.8m/s and 933.6m/s with thicknesses of 2.5m and 23.7m respectively.

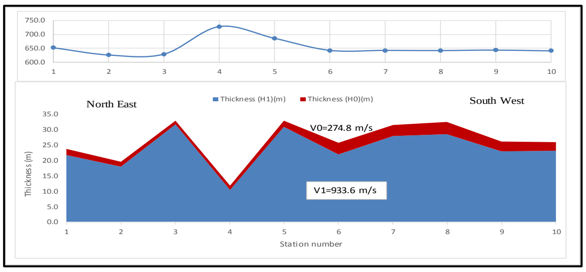


**Fig. 9:** *LVL and topography variation along line 7*

Lines 3, 4 5 and 6 (Fig. 10, Fig. 11, Fig.12 and Fig. 13) are oriented in east-west direction. The elevation in lines 3, 4 and 5 decreases towards the west as shown in Fig. 10, Fig. 11 and Fig. 12. Line 3 is at the extreme south and cuts through swampy regions of Shompole (Fig.3). Lines 4 and 5 go through Lake Magadi. The LVL of line 3 decreases towards East (Fig. 10). It has the least LVL with layer 1 and 2 having thickness of 1.6m and 16m with average velocities of 328.7m/s and 956.8m/s. The LVL decreases gently westwards which is similar to elevation. Station 1 has the maximum thickness along the profile while stations 7 and 9 have the least depth

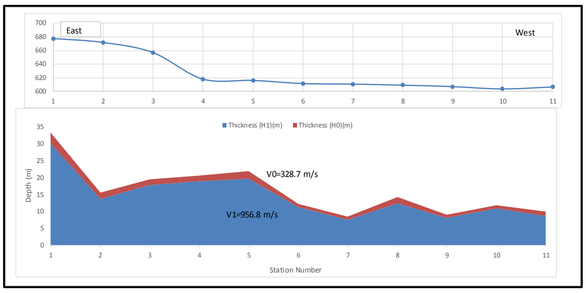


**Fig. 10**: *LVL and elevation variation along line 3*

The thickness of LVL of line 4 (Fig. 11) decreases towards the west with higher thickness observed between stations 1-6 and 11, while stations 7, 10 and 14 have the least thickness. The average thickness of layer 1 is 3.2m while layer 2 is 23.7m. The velocity of layer 1 is 311.8m/s while layer 2 is 1134.4m/s; which all lie within the velocity of weathering zone.

Line 5 cuts through Lake Magadi and the thickness of LVL increases westwards as well as the elevation as seen in Fig. 12. LVL is thicker between stations 1 and 8 approximately 33m. Station 5-8 lies within the Lake Magadi and has the maximum depth. Beyond station 8, the thickness reduces to about 25m while the elevation tends to a constant. The average thickness of layer 1 is 3.6m while layer 2 is 30.8m. The average velocity for this line is 323m/s for layer 1 and 997m/s for layer 2 (Fig. 12). These larger thickness and low velocity in this line could be attributed to volcanic sediments mainly deposited cherts, clays, alluvial silts and trona which is dominant in the area and has been carried by run off and to a lesser extent wind erosion and later deposited into the lake.

Line 6 (Fig. 13) oriented westwards has maximum LVL thickness at station 4. Layer 1 has high thickness between stations 3-5, which is also observed in layer 2. The velocity of the first layer is 381 m/s and 1059 m/s for the second layer. The depth averages to 3.2m for the first layer and 20.4m for the second layer resulting in average thickness 23.6m of the weathered layer.

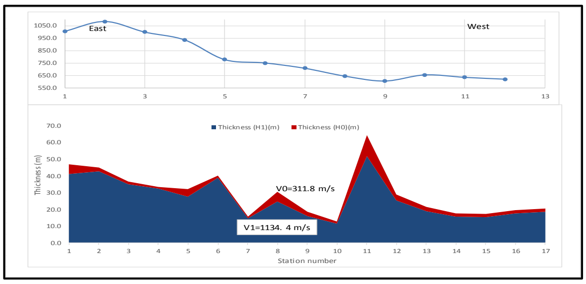


**Fig. 11**: *Topography and LVL variation along line 4*

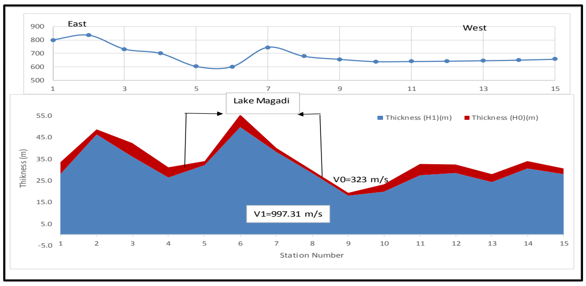


**Fig. 12**: *Elevation and LVL variation along line 5*

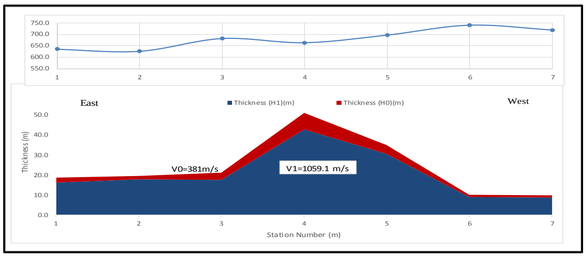


**Fig. 13**: *LVL and elevation variation along line 6*

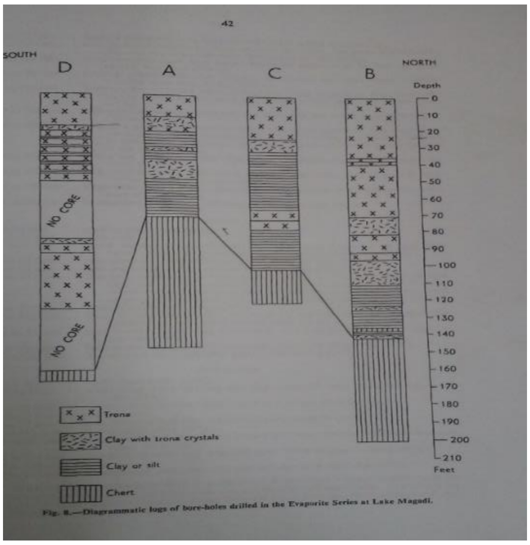


**Fig 14:** *Borehole logs drilled in Lake Magadi [11]*

The LVL of Magadi basin is basically made of two layers. This layers are composed of trona, clay, silts, mud and cherts [11]. Trona is the main rock found within Lake Magadi and in the first layer resulting in low velocities experienced in line 4, 5 and 6 (Fig. 11, Fig. 12 and Fig. 13). Though, silts and mud forms highest percentage of layer 1 in the lake, cherts and clay forms the highest percentage part of layer 2 in the Lake (Fig. 14). Further, the outflowing of volcanic rock from the surrounding hot spring could aid in transportation of this sediments resulting in increased size of the LVZ. Studies by Komolafe et al., [17] to identify faults and fractures by resistivity and other methods showed weathered zone of about 25-32m. This results do concur with the average LVL thickness of most profiles. Regions beyond Lake Magadi are made of volcanic trachytes and cherts forming the most of the low velocity layer.

## V. CONCLUSION

The study reveals that weathering thickness generally decreases towards the south as well as elevation. Surface run off, hill wash and normal erosion on the surface allowed for more deposition of sediments in the Lake Magadi and the surrounding regions thereby significantly increasing the thickness of the weathered zone in this regions. Further, the low velocities observed on semi-weathered zone could also be an effect of hydrothermal–saline conditions and reworked or sheared sediments consisting of clay, trachytes and mud. This fragmented sediments of mud, clay and trachytes leads to low velocities in the weathered and semi-weathered layer. A two layer model of the low velocity zone is obtained; the weathered zone and the semi-weathered zone. The third layer which is consolidated/ bedrock zone is only observed from the velocities. Line 3 has the least LVL of approximately 16m and while line 5 is the thickest about 34.4m. Layer 1 of line 6 has the highest average velocity of 381 m/s while layer 1 of line 1 has the lowest velocity of 262.6 m/s. Layer 2 of line 2 has the highest velocity of 1328.8 m/s while that of line 8 has the least velocity of 878.2 m/s showing LVL of Magadi basin lies within the weathered zone of less than 1500 m/s. These results show that the weathering zone could result in adverse effect on deeper reflection seismic data since it exists in Magadi basin. Therefore, this region requires static correction to be applied when processing deep seismic reflection data. The study also recommends uphole survey to be carried in the area so that uphole data can beef up shallow refraction survey. Core samples can be obtained from uphole survey for further analysis to get the lithological characteristics of the low velocity layer in other parts of Magadi Basin. For processing of deep seismic reflection survey in Magadi basin, substantial static corrections due to the high variability of weathered layer, its velocity and elevation should be done for better identification of structural and lithological features for hydrocarbon identification

## REFERENCES

[1] Krisp Working Group, “Structure of the Kenyan Rift from seismic Refraction”, Nature, 1987, 325, pp. 239-242.

[2] J. Mechie, G.R. Keller, L.W. Braile, W.D. Mooney and C. Prodehl, “Structure of the Uppermost Mantle beneath the Kenya Rift,” Tectonophysics, 1994, 236, pp. 201-216.

[3] K.P. Bonjer, K. Fuchs and J. Wohlenberg, “Crustal Structure of the East African Rift System from Spectral Response Ratios of long Period body waves”, Journal of Geophysics,1970, 46, pp. 287-297.

[4] R.W. Backhouse and R.E. Long, “The structure of the Western flank of the Gregory Rift, Part 1. The Mantle”, Geophysical Journal International, 1976, 44(3), pp. 677-688.

[5] J.G. Githiri, “Gravity and Magnetic Investigations of the Greater Magadi area in Kenya”, Journal of Agriculture Science and Technology, 2009, 14(1), pp. 142-160.

[6] P. Docherty, “Solving for the Thickness and Velocity of the Weathering Layer Using 2-D Refraction Tomography”, Geophysics Journal, 1992, 57(10), pp. 1307-1318.

[7] C.D. Lawton, “Computation of refraction static using first-break travel time differences”, Geophysics, 1989, 54(10), pp. 1289-1296.

[8] F. Kolawole, C. Okror and O.P. Olaleye, “Downhole Refraction Survey in Niger Delta Basin: A 3-layer Model”, APRN Journal of Earth Sciences, 2012, 1(2), pp. 67-79.

[9] S. Saha, A. Mandal, B. Borah and M. Gupta, “Characteristics of Low Velocity Layer in Upper Assam Basin near Naga Thrust: A brief Study”, 9th Biennial International Conference and Exposition on Petroleum Geophysics, Hyderabad, 2012, pp. 249-253.

[10] B. Baker, “Geology of the Magadi area, report. Geological survey of Kenya 42”. The government Printer, Nairobi, 1958.

[11] B. Baker, “Geology of the area of South Magadi, report. Geological survey of Kenya 61”. The government Printer, Nairobi, 1963.

[12] R. Crossley, “Structure and Volcanism in the Southern Kenya Rift. In Geodynamic evolution of the Afro-Arabian Rift system”, Academic, 1979, pp. 89-98.

[13] D. Riaroh and W. Okoth, “The geothermal fields of the Kenya Rift”, Tectonophysics, 1994, 236(2), pp. 117-130.

[14] P. Keary, M. Brooks and I. Hill, An introduction to Geophysical Exploration. Blackwell Scientific Publications, 2005.

[15] K. Knödel, G. Lange and H.N. Voigt, Environmental Geology: Handbook of Field Methods and Case Studies, Springer. Verlag: Berlin Heidelberg, 2007.

[16] A.A. Komolafe, Z.N. Kuria, T. Wolda, M. Noomen, and A.Y.B. Anifowose, “Integrated Remote Sensing and Geophysical Investigations of the Geodynamic Activities at Lake Magadi, Southern Kenyan Rift”, International Journal of Geophysics, 2012.